

State transfer with separable optical beams and variational quantum algorithms with classical light

SOORYANSH ASTHANA^{1,*} AND V. RAVISHANKAR^{1,†}

¹Department of Physics, Indian Institute of Technology Delhi, New Delhi, 110016, India.

*sooryansh.asthana@physics.iitd.ac.in

†vravi@physics.iitd.ac.in

Compiled March 19, 2022

Classical electromagnetic fields and quantum mechanics—both obey the principle of superposition alike. This opens up many avenues for simulation of a large variety of phenomena and algorithms, which have hitherto been considered quantum mechanical. In this paper, we propose two such applications. In the first, we introduce a new class of beams, called equivalent optical beams, in parallel with equivalent states introduced in [Bharath & Ravishankar, *Phys. Rev. A* 89, 062110]. These beams have the same information content for all practical purposes. Employing them, we show how to transfer information from one degree of freedom of classical light to another, without any need for classically entangled beams. Next, we show that quantum machine learning can be performed with OAM beams through the implementation of a quantum classifier circuit. We provide explicit protocols and experimental setups for both the applications.

© 2022 Optical Society of America

OCIS codes: (000.1600) Classical and quantum physics (270.0270) Coherence (200.3050) Information processing (270.5585) Quantum information and processing

<http://dx.doi.org/10.1364/ao.XX.XXXXXX>

1. INTRODUCTION

Recent times have witnessed a surge of interest in quantum algorithms and quantum foundations. This has culminated in quantum computing algorithms [1–4], quantum factorisation algorithm [5], quantum search algorithm [6] and variational quantum algorithms [7–11]. The reason for quantum speedups in these algorithms has been a matter of intense research so as to identify appropriate resource states. This, in turn, has led to significant developments in resource theories of quantum entanglement [12], quantum coherence [13], quantum discord [14], quantum contextuality [15], etc. From the viewpoint of quantum foundations, it is of paramount importance to differentiate the effects that are exclusively quantum mechanical vis-a-vis that can be simulated by some classical systems [16].

In parallel, there have been remarkable developments in generation, manipulation and detection of orbital angular momentum (OAM) modes of light [17–20]. These modes have found applications in diverse fields, e.g., optical tweezers, microscopy and imaging (see [21] and references therein). Of particular importance to us are the following two facts: (I) a classical beam carrying OAM of light provides an experimental demonstration of a higher dimensional system obeying the principle of superposition, and, more significantly, (II) $SU(2)$ coherent OAM beams have been experimentally generated in [22]. These beams

are classical counterparts of $SU(2)$ coherent states in quantum mechanics.

In classical computation, there is no difference between N bits and a single dit with $d = 2^N$, as far as algebraic manipulations are concerned. So, the representations in different number systems, e.g., binary, octal, decimal and hexadecimal systems can be freely converted to one another. The situation changes in quantum computation due to the principle of superposition. Additionally, in the quantum realm, two subsystems of entangled states may be at different locations. Barring that, classical waves and quantum systems share common features.

A systematic study of those features, that are shared with classical systems, bears a twofold advantage. From the foundational perspective, it bifurcates the exclusively-quantum mechanical features and the quantum mechanical features shared by some classical systems as well. From the viewpoint of applications, this study provides us with various platforms for implementation of many quantum algorithms and protocols, say, with OAM modes of classical light. For example, hybrid modes of OAM provide a physical example of classically entangled beams as they also carry polarisation. In fact, electromagnetic fields have different physical properties associated with them. Interference involving these degrees of freedom has been demonstrated in [23–27]. For example, a two-dimensional Hilbert space in quantum mechanics shares a formal equivalence with a two-

dimensional space spanned by the two orthogonal polarisations of the classical light. OAM modes of light [28] form a theoretically unbounded space with discrete indices. The coherent mode representation of partially coherent light fields is formally equivalent to the density matrix in quantum mechanics [25].

This suggests that those quantum phenomena or algorithms, that have their geneses in parallelism and entanglement at one spatial location [29], can also be implemented with classical electromagnetic waves. It has led to an ongoing interest to implement quantum algorithms and protocols with orbital angular momentum modes of classical light. For example, in [30], classical analogue of quantum teleportation has been demonstrated for transfer of information from OAM to polarisation degree of freedom of a beam. In [31], monogamy relation between contextuality and nonlocality in quantum theory has been simulated in classical optical systems. It has been performed by using polarization, path, and OAM of a classical optical beam. Quantum random walk has been implemented in [32], by employing OAM and polarisation degrees of freedom of classical light. The proposed experimental setups accomplish the same task without the need for a single photon source, which is hard to prepare [33]. There are many more quantum phenomena and algorithms that have been simulated with classical light, but not necessarily with OAM modes [34–42]. For a detailed review of classical entanglement, one may refer to [29] and references therein. We refer the reader to [40] for a discussion of quantum mechanics and classical electromagnetic theory.

In this paper, we take a step ahead and ask if there can be a further simplification. We start with the question: whether classically entangled beams can themselves be replaced by classically separable beams in information theoretic processes, perhaps, in higher dimensions? By classically separable beams, we mean those beams that can be obtained as incoherent superpositions of pure separable beams. To answer this question, we first introduce equivalent beams, analogous to equivalent states, proposed in [43] in the quantum domain. Equivalent beams are best understood through $SU(2)$ -coherent beams. $SU(2)$ coherent beams share all the properties of $SU(2)$ coherent states. These beams have been experimentally realised recently with OAM modes [22]. The set of $SU(2)$ -coherent beams forms an overcomplete basis. So, any beam can be expanded in this basis. The expansion of any beam in this basis is termed as its Q -representation. Two optical beams are recognized to be *equivalent* if they share the same Q -representation. Interestingly, the higher-dimensional (e.g., OAM) equivalent beams of a pure lower dimensional (e.g., fully polarised) beam turn out to be highly mixed. More importantly, the equivalent beams of a lower dimensional classically entangled beam can, in fact, be separable. Thus, this formalism provides us with a tool to harness highly mixed separable states for information processing.

As an application of this formalism, we propose a protocol for transferring information from the path degree of freedom to the OAM degree of freedom of a classical beam. This protocol is the classical optical version of a protocol, recently proposed by us in [44] in the quantum realm. Due to experimental advancements in generation, manipulation and detection of OAM modes [17–20], this protocol may be easily implemented.

Many variational quantum algorithms [7–11] also require generation, manipulation and detection of quantum states, all at the same spatial location. Hence, they may also be implemented with classical optical beams. As a concrete example, we describe an experimental implementation of the quantum classifier circuit, proposed in [45], by employing OAM modes of classical

light. The experimental implementation would require a spatial light modulator [46] and a programmable hologram [47], both of which are available.

The plan of the paper is as follows: in section (2), we setup the notation to be used throughout the paper. For the sake of clarity and completion, the paper is written in somewhat pedagogical style. In section (3), the formal mapping between classical electromagnetic fields and quantum states is discussed. The central results of the paper are contained in sections (4), (5) and (8). In section (4), the concept of equivalent beams is proposed, followed by the protocol for transfer of information using separable equivalent of a classically entangled beam in section (5). In section (6), we show how information transfer can be accomplished between different degrees of freedom of a noisy beam, by employing a detector with higher resolution for its retrieval. Sections (7) and (8) discuss simulability of a variational quantum algorithm with OAM modes of classical light. Section (9) summarises the paper with concluding remarks.

2. NOTATION

We first setup the notation for an uncluttered discussion.

1. Following [48], we employ $|\rangle$ and $\langle|$ for classical optical beams, in place of ket and bra respectively, in order to avoid confusion. We employ Dirac's Bra-Ket notation for quantum mechanical states.
2. We use the symbol J for coherent mode representation of classical beams and reserve the symbol ρ exclusively for quantum mechanical density matrices. The superscript of J represents the degree of freedom which the coherent mode representation belongs to, which will be clear from the context.
3. The symbol $|LG_{pl}\rangle$ is used for Laguerre-Gauss modes with the radial mode index p and the azimuthal mode index l .
4. The generators of $SU(2)$ in any dimension will be represented by T_1, T_2 and T_3 . In two dimensions, the generators T_i have the form $T_i \equiv \frac{\sigma_i}{2}$, where σ_i are Pauli matrices.
5. We shall, henceforth, employ the following two shorthand notations, in order to avoid mathematical clutter:

$$\vec{T} \cdot \vec{m} \equiv T_1 m_1 + T_2 m_2 + T_3 m_3,$$

$$\sum_{i=1}^3 T_i^A \otimes T_i^B \equiv \vec{T}^A \cdot \vec{T}^B \equiv T_1^A T_1^B + T_2^A T_2^B + T_3^A T_3^B, \quad (1)$$

where m_1, m_2, m_3 are components of \vec{m} along three mutually orthonormal directions \hat{e}_1, \hat{e}_2 and \hat{e}_3 respectively. In the quantum domain, the symbols A and B can represent two subsystems of the same system whereas for a classical light, they only represent two degrees of freedom of a light beam. For example, A and B may represent polarisation and OAM degrees of freedom.

3. FORMAL EQUIVALENCE BETWEEN QUANTUM MECHANICAL STATES AND CLASSICAL ELECTROMAGNETIC FIELDS

We briefly recapitulate the polarisation matrix of a classical electromagnetic field, given in [23, 25]. We represent the coordinates

of the electric field associated with a quasimonochromatic plane wave ($z = 0$), in terms of a row vector as,

$$\mathbf{E} = E_x(t)\hat{x} + E_y(t)\hat{y} \mapsto (E_x(t), E_y(t)). \quad (2)$$

If the field is not completely coherent, we can represent it in terms of a 2×2 density matrix J , termed as the *polarisation matrix*. In the $x - y$ coordinate system, it takes the following form,

$$J^{\text{pol}} = \frac{1}{I} \begin{pmatrix} J_{xx} & J_{xy} \\ J_{yx} & J_{yy} \end{pmatrix} = \frac{1}{I} \begin{pmatrix} \langle E_x^*(t)E_x(t) \rangle & \langle E_x^*(t)E_y(t) \rangle \\ \langle E_y^*(t)E_x(t) \rangle & \langle E_y^*(t)E_y(t) \rangle \end{pmatrix}. \quad (3)$$

The angular bracket $\langle \cdot \rangle$ represents the time-average and I represents the total intensity. Note that the polarisation matrix, J^{pol} , is a positive-semidefinite hermitian matrix with unit trace. So, in its eigen-basis, the matrix J^{pol} can be resolved as an incoherent sum of two coherent modes. If it represents a fully coherent field, one of the eigenvalues vanishes.

A. Formal analogy between polarisation matrix of classical light and a qubit: coherent mode representation

In classical electromagnetic fields, all the components of the fields are, in principle, completely measurable. Quantum mechanics, however, starts with probability amplitudes, whose bilinears are measurable. For clarity and pedagogical purpose, it is, therefore, worthwhile to establish what the formal equivalence between the two is.

Fully and partially coherent electromagnetic fields are formally equivalent to pure states and mixed states in quantum mechanics respectively. It is, however, crucial to note that this mapping is purely formal in the sense that quantum mechanical probability amplitudes map to the amplitudes of electromagnetic fields. Quantum mechanical probabilities, intrinsic to quantum mechanics, map to normalised intensities of the electromagnetic fields. We, thus, recognise that J^{pol} has the same structure as that of the density matrix of a qubit, though the underlying physical quantities are completely different (for an illuminating discussion of partially polarised light, we refer the reader to [49]).

A.1. c-Entropy as a quantifier of degree of polarisation

Since probability in quantum mechanics maps to normalised intensity of an electromagnetic field, all the functions of quantum probability naturally map to corresponding functions of normalised intensity. So, the classical counterpart of von-Neumann entropy $S(\rho) = -\text{tr}(\rho \log \rho)$ of a qubit ρ , is given by a function, that we term as *c-entropy*,

$$S(J^{\text{pol}}) = -\text{tr}(J^{\text{pol}} \log J^{\text{pol}}). \quad (4)$$

For J^{pol} , the function $S(J^{\text{pol}})$ is decreasingly monotonic with degree of polarisation.

4. EQUIVALENT STATES AND EQUIVALENT BEAMS

This section contains a central result of the paper. In this section, we address the question: whether classically entangled beams can themselves be mimicked by classically separable beams? As mentioned in section (1), by classically separable beams, we mean those beams that can be written as incoherent superpositions of pure separable beams. To answer this question, we

introduce a concept of equivalent beams. This, in turn, is based on the concept of equivalent states, introduced in [43]. Equivalent separable beams of classically entangled beams generally exist in higher dimensions and can be highly mixed. We shall show that the equivalent separable beams can be written as incoherent superpositions of $SU(2)$ coherent beams. Experimental preparation of equivalent beams of a 2×2 classically entangled beam is feasible because $SU(2)$ coherent beams have already been experimentally realised in the OAM domain [22]. Interestingly, it is an area in which a quantum mechanical concept enriches the understanding in the classical domain.

We start with a brief recapitulation of equivalent states with the examples of single qubit and two-qubit states. For a detailed discussion, one can refer to [43]. For a discussion of separable equivalent states of higher dimensional entangled states, we refer the reader to [50].

A. Q-representation and equivalent states in the quantum domain

A.1. Q-representation of a quantum state

In quantum mechanics, a $SU(2)$ -coherent state $|\hat{n}(\theta, \phi)\rangle$ (originally introduced for spin systems) is generated by the operation of $(2T + 1)$ -dimensional irreducible representation of the rotation group, $SU(2)$, on the state $|T_3 = +T\rangle$ [51]. That is to say,

$$|\hat{n}(\theta, \phi)\rangle = e^{-iT_3\phi} e^{-iT_2\theta} e^{-iT_1\psi} |T_3 = +T\rangle, \quad (5)$$

where T_1, T_2, T_3 are the generators of $SU(2)$ in $(2T + 1)$ dimensions. ψ is an uninteresting overall phase. The set of $SU(2)$ -coherent states $\{|\hat{n}(\theta, \phi)\rangle\}$ forms an overcomplete set, i.e.,

$$\frac{2T + 1}{4\pi} \int \sin \theta d\theta d\phi |\hat{n}(\theta, \phi)\rangle \langle \hat{n}(\theta, \phi)| = 1. \quad (6)$$

Thus, a density matrix ρ can be expanded in this overcomplete basis. The Q -function of a density matrix ρ , denoted by $F(\hat{n})$, is defined as,

$$F(\hat{n}) = \frac{2T + 1}{4\pi} \langle \hat{n}(\theta, \phi) | \rho | \hat{n}(\theta, \phi) \rangle. \quad (7)$$

Due to the overcompleteness property of $SU(2)$ -coherent states, $F(\hat{n})$ completely determines the density matrix ρ .

A.2. Equivalent states

Let there be two states ρ_1 and ρ_2 , belonging to the Hilbert spaces, \mathcal{H}^{d_1} and \mathcal{H}^{d_2} , of dimensions d_1 and d_2 respectively. The states ρ_1 and ρ_2 are termed as *equivalent* if they share the same Q -representation [43]. For example, a qubit density matrix $\rho^{1/2}(\vec{p}) = \frac{1}{2}(\mathbb{1} + \vec{\sigma} \cdot \vec{p})$ has the following $(2T + 1)$ -dimensional equivalent,

$$\rho^T(\vec{p}) = \frac{1}{2T + 1}(\mathbb{1} + \hat{T} \cdot \vec{p}), \quad \hat{T} = \frac{\vec{T}}{T}. \quad (8)$$

Evidently, states equivalent to a pure qubit state are all mixed. It is obvious from equation (8) that, for $T = \frac{1}{2}$ and $|\vec{p}| = 1$, the state $\rho^{1/2}(\vec{p})$ is pure, whereas for all higher T values, it is mixed. The crucial point is that the family of states $\rho^T(\vec{p})$ have one and the same Q -function, given by,

$$F(\hat{n}) = \frac{1}{4\pi}(1 + \vec{p} \cdot \hat{n}). \quad (9)$$

Equivalent states have the same information content and hence, they are equally good resources for information processing. In order to extract that information, the concept of equivalent observables is introduced below.

A.3. Equivalent observables

Let $\rho_1 \in \mathcal{H}^{d_1}$ and $\rho_2 \in \mathcal{H}^{d_2}$ be two equivalent states. The observables $\hat{O} \in \mathcal{H}^{d_1}$ and $\hat{O}' \in \mathcal{H}^{d_2}$ are termed as equivalent observables if,

$$\text{Tr}(\rho_1 \hat{O}) = \text{Tr}(\rho_2 \hat{O}'). \quad (10)$$

For example, the observable $\hat{O} \equiv \vec{\sigma} \cdot \hat{m}$ for a qubit has its equivalent observable $\hat{O}' \equiv \frac{3T}{T+1} \hat{T} \cdot \hat{m}$ belonging to a $(2T+1)$ -dimensional space.

We now turn our attention to two-qubit systems. The most general density matrix of a two-qubit system is written as,

$$\rho^{\frac{1}{2}, \frac{1}{2}} = \frac{1}{4} [\mathbb{1} + \vec{\sigma}^A \cdot \vec{p} + \vec{\sigma}^B \cdot \vec{q} + t_{ij} \sigma_i^A \sigma_j^B]. \quad (11)$$

Its $\frac{1}{2} \otimes T$ -equivalent state is given by,

$$\rho^{\frac{1}{2}, T} = \frac{1}{2(2T+1)} [\mathbb{1} + \vec{\sigma}^A \cdot \vec{p} + \hat{T}^B \cdot \vec{q} + t_{ij} \sigma_i^A \hat{T}_j^B], \quad \hat{T}^B = \frac{\vec{T}}{T}. \quad (12)$$

The family of states $\rho^{\frac{1}{2}, T}$ has the same Q-representation, which is as follows:

$$F(\hat{m}, \hat{n}) = \frac{1}{(4\pi)^2} [1 + \hat{m} \cdot \vec{p} + \hat{n} \cdot \vec{q} + t_{ij} m_i n_j]. \quad (13)$$

For the special case of two-qubit Werner states,

$$\rho_W^{\frac{1}{2}, \frac{1}{2}}[\alpha] = \frac{1}{4} (\mathbb{1} - \alpha \vec{\sigma}^A \cdot \vec{\sigma}^B), \quad \alpha \in \left[-\frac{1}{3}, 1\right], \quad (14)$$

the equivalent $\frac{1}{2} \otimes T$ states are given by,

$$\rho_W^{\frac{1}{2}, T}[\alpha] = \frac{1}{2(2T+1)} (\mathbb{1} - \alpha \vec{\sigma}^A \cdot \hat{T}^B), \quad \alpha \in \left[-\frac{T}{T+1}, 1\right]. \quad (15)$$

Crucially, the state $\rho_W^{\frac{1}{2}, T}[\alpha]$ is separable in the range,

$$|\alpha| \leq \frac{T}{T+1}. \quad (16)$$

It implies that a lower dimensional entangled state can have higher dimensional separable states as its equivalents. This phenomenon has been termed as ‘classical simulation of entangled states’. The minimum value of T , for which the $\frac{1}{2} \otimes T$ separable equivalents of two-qubit Werner states exist, can be obtained from equation (16). If we denote the minimum value of T by T_{\min} , it is given by the minimum half-integer or integer greater than $\frac{|\alpha|}{1-|\alpha|}$. We consider a few values of α and find out the corresponding T_{\min} as follows:

1. For $\alpha = 0.5$, $T_{\min} = 1$, i.e., the equivalent separable state belongs to a three-dimensional Hilbert space.
2. For $\alpha = 1$, i.e., for the pure Bell state, the equivalent separable state belongs to the infinite dimensional Hilbert space.

So, for $\alpha \neq 1$, separable equivalent states belong to finite dimensional Hilbert spaces. The equivalent higher dimensional separable states yield, in principle, the same advantage as the lower dimensional entangled states. For this reason, they can be harnessed in information processing tasks. Some applications of the equivalent separable states in quantum communication protocols have been shown in [44].

The degree of mixedness of the family of states, given in (15), is given by the quantity $1 - \text{Tr}(\rho_W^{\frac{1}{2}, T}[\alpha])^2$, which in terms of α and T is given as,

$$\mathcal{M} \equiv 1 - \text{Tr}(\rho_W^{\frac{1}{2}, T}[\alpha])^2 = \frac{1}{4(2T+1)} (4(2T+1) - 2 - \alpha^2 \frac{T+1}{T}), \quad (17)$$

So, for a given value of α , the degree of mixedness \mathcal{M} increases as T increases. It is reflected by the derivative,

$$\frac{d\mathcal{M}}{dT} = \frac{\alpha^2(2T^2 + 4T + 1)}{4T^2(2T+1)^2} + \frac{1}{(2T+1)^2}, \quad (18)$$

which is always positive. So, information processing with equivalent separable states yields a two-fold advantage: it allows for information processing with mixed states, which are separable as well. Of course, the proposed protocols do not yield 100% fidelity as the equivalent separable state of a pure Bell state belongs to the infinite dimensional Hilbert space.

B. Q-representation and equivalent beams in the classical domain

We are in a position to advance the concept of equivalent beams. Different degrees of freedoms of optical beams, e.g., polarisation and OAM form Hilbert spaces. So, the concept of equivalence is amenable to light beams as well.

B.1. $SU(2)$ coherent optical beams

The classical counterpart of a $SU(2)$ coherent state is a $SU(2)$ coherent optical beam, defined by [22],

$$|\hat{n}(\theta, \phi)\rangle = e^{-iT_3\phi} e^{-iT_2\theta} e^{-iT_3\psi} |T_3 = +T\rangle. \quad (19)$$

T_1, T_2 and T_3 are generators of $SU(2)$ in $(2T+1)$ -dimensional space, defined with respect to a convenient basis consisting of orthonormal modes of electromagnetic beams. The physical significance of T_1, T_2, T_3 depends on the context. The beam $|T_3 = +T\rangle$ corresponds to the eigenfunction of T_3 with the highest eigenvalue and the unit vector \hat{n} is given by,

$$\hat{n} \equiv \sin \theta \cos \phi \hat{e}_1 + \sin \theta \sin \phi \hat{e}_2 + \cos \theta \hat{e}_3, \quad (20)$$

where \hat{e}_1, \hat{e}_2 and \hat{e}_3 are mutually orthonormal unit vectors.

As an illustration, if we take a three-dimensional Hilbert space spanned by three Laguerre Gauss modes $|LG_{0-1}\rangle, |LG_{00}\rangle, |LG_{01}\rangle$ and identify them with respective eigenstates of T_3 , the matrix representations of T_1 and T_2 have the following forms:

$$T_1 = \begin{pmatrix} |LG_{0-1}\rangle & |LG_{00}\rangle & |LG_{01}\rangle \\ \langle LG_{0-1}| & \langle LG_{00}| & \langle LG_{01}| \end{pmatrix} \begin{pmatrix} 0 & \frac{1}{\sqrt{2}} & 0 \\ \frac{1}{\sqrt{2}} & 0 & \frac{1}{\sqrt{2}} \\ 0 & \frac{1}{\sqrt{2}} & 0 \end{pmatrix}$$

$$T_2 = \begin{pmatrix} |LG_{0-1}\rangle & |LG_{00}\rangle & |LG_{01}\rangle \\ \langle LG_{0-1}| & \langle LG_{00}| & \langle LG_{01}| \end{pmatrix} \begin{pmatrix} 0 & -\frac{i}{\sqrt{2}} & 0 \\ \frac{i}{\sqrt{2}} & 0 & -\frac{i}{\sqrt{2}} \\ 0 & \frac{i}{\sqrt{2}} & 0 \end{pmatrix}. \quad (21)$$

The $SU(2)$ -coherent optical beam $|\hat{n}(\theta, \phi)\rangle$ would have the following form,

$$\begin{aligned} |\hat{n}(\theta, \phi)\rangle &= e^{-iT_3\phi} e^{-iT_2\theta} |\text{LG}_{01}\rangle \\ &= \frac{1}{2} e^{i\phi} (1 - \cos\theta) |\text{LG}_{0-1}\rangle - \frac{\sin\theta}{\sqrt{2}} |\text{LG}_{00}\rangle \\ &\quad + \frac{1}{2} e^{-i\phi} (1 + \cos\theta) |\text{LG}_{01}\rangle. \end{aligned} \quad (22)$$

We note that the physical significance of T_1 , T_2 and T_3 depends on the basis chosen and the manner in which they are ordered. It is of great interest and importance for us to see the intensity profiles of these beams. We show some characteristic profiles of the beams $|\hat{n}(\theta, \phi)\rangle$ for $\theta = \frac{\pi}{4}, \frac{\pi}{3}, \frac{\pi}{2}$ and $\phi = 0, \frac{\pi}{4}, \frac{\pi}{2}, \frac{3\pi}{4}, \pi$, in transverse planes, in figures (1), (2) and (3).

Similarly, $SU(2)$ -coherent optical beams $|\hat{n}(\theta, \phi)\rangle$ can be constructed in higher dimensions. These beams have been realised experimentally upto eight dimensions in [22], by employing astigmatic mode transformations of geometric modes generated by Nd-YAG laser.

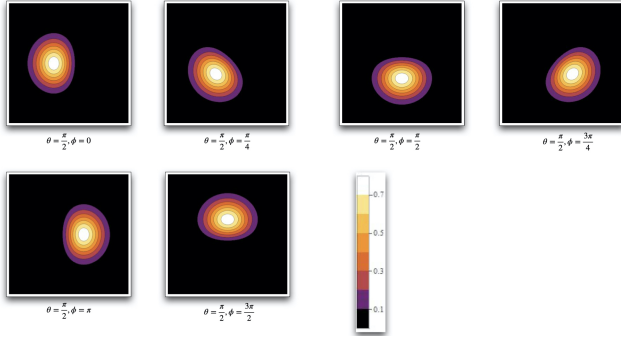


Fig. 1. Intensity of $SU(2)$ coherent beam corresponding to $\theta = \frac{\pi}{2}$ and different values of ϕ .

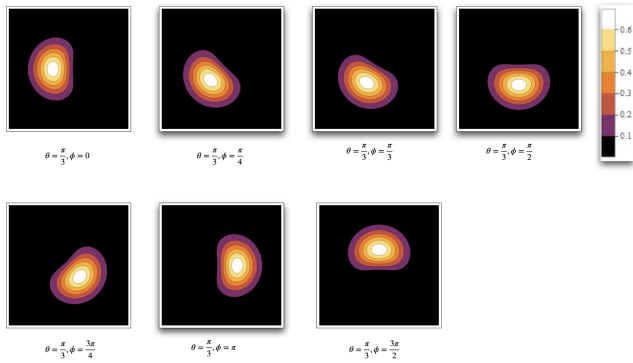


Fig. 2. Intensity of $SU(2)$ coherent beam corresponding to $\theta = \frac{\pi}{3}$ and different values of ϕ .

B.2. Q-representation of an optical beam

The set of $SU(2)$ -coherent beams $\{|\hat{n}(\theta, \phi)\rangle\}$ forms an overcomplete set, i.e.,

$$\frac{2T+1}{4\pi} \int \sin\theta d\theta d\phi |\hat{n}(\theta, \phi)\rangle \langle \hat{n}(\theta, \phi)| = \mathbb{1}. \quad (23)$$

Thus, any optical beam, whose coherent mode representation is given by a matrix J , can be expanded in this overcomplete

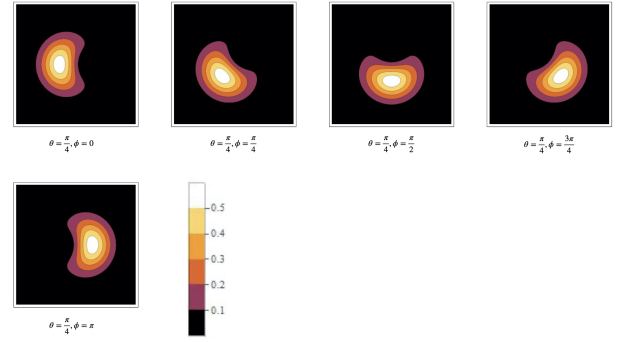


Fig. 3. Intensity of $SU(2)$ coherent beam corresponding to $\theta = \frac{\pi}{4}$ and different values of ϕ .

basis provided by $\{|\hat{n}(\theta, \phi)\rangle\}$. The corresponding Q-function, denoted by $F(\hat{n})$, is simply defined as,

$$F(\hat{n}) = \frac{2T+1}{4\pi} \langle \hat{n}(\theta, \phi) | J | \hat{n}(\theta, \phi) \rangle. \quad (24)$$

Due to overcompleteness, the diagonal elements $\langle \hat{n}(\theta, \phi) | J | \hat{n}(\theta, \phi) \rangle$ completely determine the matrix J . Thus, the complete information of the beam is mapped to a single function $F(\hat{n})$, defined on a sphere.

B.3. Equivalent beams

Let J_1 and J_2 be coherent mode representations of two beams (or of two degrees of freedom of the same beam) belonging to Hilbert spaces of dimensions d_1 and d_2 respectively. The two beams are termed as *equivalent* if they share the same Q-representation. For example, a polarisation matrix $J^{1/2}(\vec{p}) = \frac{1}{2} (\mathbb{1} + \vec{\sigma} \cdot \vec{p})$ has the following $(2T+1)$ -dimensional equivalent beams whose coherent mode representations are given by,

$$J^T(\vec{p}) = \frac{1}{2T+1} (\mathbb{1} + \hat{T} \cdot \vec{p}), \quad \hat{T} = \frac{\vec{T}}{T}. \quad (25)$$

Interestingly, completely polarised beams have higher dimensional mixed beams as their equivalents. The Q-representation of the beams $J^T(\vec{p})$ is given by $F(\hat{n}) = \frac{1}{4\pi} (1 + \vec{p} \cdot \hat{n})$.

The spectral decompositions of equivalent OAM beams of fully polarised light with the choice, $\vec{p} = (0, 0, 1)^T$, belonging to three and five dimensional Hilbert spaces, are shown in figures (4) and (5) respectively. We have also shown the intensities of the corresponding OAM beams in transverse planes that can be observed in experiments.

B.4. Equivalent observables for equivalent beams

Equivalent observables for equivalent beams can be defined in a similar way, as in the quantum case, with the sole provision that probability maps to the normalised intensity. As an example, the two-dimensional observable $\vec{\sigma} \cdot \vec{m}$ maps to the observable $\frac{3T}{T+1} \hat{T} \cdot \vec{m}$ in $(2T+1)$ dimensions.

As an illustration, let a three-dimensional Hilbert space be spanned by the modes $\{|\text{LG}_{0-1}\rangle, |\text{LG}_{00}\rangle, |\text{LG}_{01}\rangle\}$. For the particular choice of,

$$\hat{m} = \sin\alpha \cos\beta \hat{e}_1 + \sin\alpha \sin\beta \hat{e}_2 + \cos\alpha \hat{e}_3, \quad |\hat{e}_1 \cdot (\hat{e}_2 \times \hat{e}_3)| = 1, \quad (26)$$

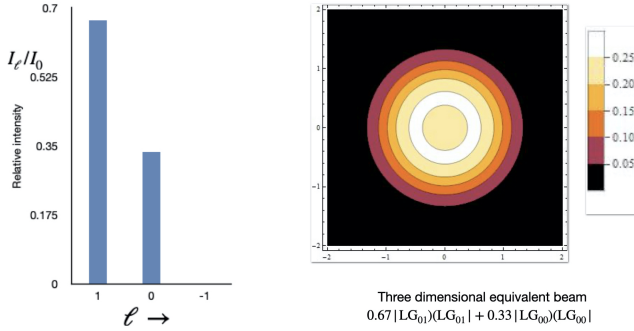


Fig. 4. Spectral decomposition of a three dimensional equivalent beam of a pure two dimensional beam. For example, the three dimensional beam may be an OAM beam belonging to the Hilbert space spanned by $\{|LG_{0-1}\rangle, |LG_{00}\rangle, |LG_{01}\rangle\}$ and the two dimensional pure beam may correspond to a fully polarised beam.

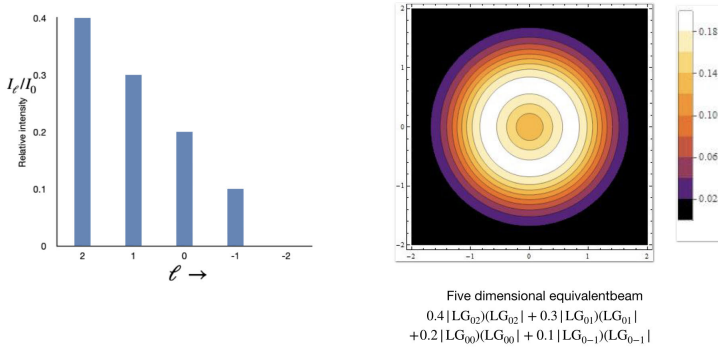


Fig. 5. Spectral decomposition of a five dimensional equivalent beam of a pure two dimensional beam. For example, the five dimensional beam may be an OAM beam belonging to the Hilbert space spanned by $\{|LG_{0-2}\rangle, |LG_{0-1}\rangle, |LG_{00}\rangle, |LG_{01}\rangle, |LG_{02}\rangle\}$ and the two dimensional pure beam may correspond to a fully polarised beam.

the matrix representation of the observable $\frac{3T}{T+1} \hat{T} \cdot \vec{m}$ in this Hilbert space is given by,

$$\frac{3T}{T+1} \hat{T} \cdot \vec{m} \Big|_{T=1} = \frac{3}{2} \begin{pmatrix} -\cos \alpha & \frac{\sin \alpha e^{-i\beta}}{\sqrt{2}} & 0 \\ \frac{\sin \alpha e^{i\beta}}{\sqrt{2}} & 0 & \frac{\sin \alpha e^{-i\beta}}{\sqrt{2}} \\ 0 & \frac{\sin \alpha e^{i\beta}}{\sqrt{2}} & \cos \alpha \end{pmatrix} \quad (27)$$

The eigen-resolution of the observable, given in (27), is as follows:

$$\frac{3T}{T+1} \hat{T} \cdot \vec{m} \Big|_{T=1} = \frac{3}{2} \hat{T} \cdot \vec{m} = \frac{3}{2} (|v_1\rangle\langle v_1| - |v_2\rangle\langle v_2|), \quad (28)$$

where,

$$\begin{aligned} |v_1\rangle\langle v_1| &= \frac{1}{2} \vec{T} \cdot \vec{m} (\vec{T} \cdot \vec{m} + \mathbb{1}) \\ |v_2\rangle\langle v_2| &= \frac{1}{2} \vec{T} \cdot \vec{m} (\vec{T} \cdot \vec{m} - \mathbb{1}) \text{ and,} \\ |v_3\rangle\langle v_3| &= \mathbb{1} - (\vec{T} \cdot \vec{m})^2. \end{aligned} \quad (29)$$

So, a measurement of the observable $\frac{3}{2} \vec{T} \cdot \vec{m}$ is tantamount to measuring intensities corresponding to three one-dimensional projections $|v_1\rangle\langle v_1|$, $|v_2\rangle\langle v_2|$ and $|v_3\rangle\langle v_3|$.

B.5. Equivalents of classically entangled beams

Experimental generation of a classically entangled beam has become quite common (see, for example [29] and references therein), e.g., the beams entangled in polarisation and OAM degrees of freedom. So, in this section, we study the properties of equivalent beams of an optical beam mimicking a two-qubit system.

Let the orthonormal bases of two degrees of freedom of a beam be $\{|0\rangle_A, |1\rangle_A\}$ and $\{|0\rangle_B, |1\rangle_B\}$ respectively. The coherent mode representation of the most general beam in these two degrees of freedom is written as,

$$J^{\frac{1}{2}, \frac{1}{2}} = \frac{1}{4} [\mathbb{1} + \vec{\sigma}^A \cdot \vec{p} + \vec{\sigma}^B \cdot \vec{q} + t_{ij} \sigma_i^A \sigma_j^B], \quad i, j \in \{1, 2, 3\}, \quad (30)$$

where σ_i^A and σ_j^B represent the analogues of Pauli observables in the two degrees of freedom. The coherent mode representation of its $\frac{1}{2} \otimes T$ -equivalent beam is given by,

$$J^{\frac{1}{2}, T} = \frac{1}{2(2T+1)} [\mathbb{1} + \vec{\sigma}^A \cdot \vec{p} + \hat{T}^B \cdot \vec{q} + t_{ij} \sigma_i^A \hat{T}_j^B], \quad \hat{T}^B = \frac{\vec{T}^B}{T}. \quad (31)$$

The family of beams $J^{\frac{1}{2}, T}$ has the same Q-representation, which is as follows:

$$F(\hat{m}, \hat{n}) = \frac{1}{(4\pi)^2} [1 + \hat{m} \cdot \vec{p} + \hat{n} \cdot \vec{q} + t_{ij} m_i n_j]. \quad (32)$$

Of special interest to us is the beam, whose coherent mode representation has the same structure as Werner-states in quantum mechanics, i.e.,

$$J_W^{\frac{1}{2}, \frac{1}{2}}[\alpha] = \frac{1}{4} (\mathbb{1} - \alpha \vec{\sigma}^A \cdot \vec{\sigma}^B), \quad \alpha \in \left[-\frac{1}{3}, 1\right]. \quad (33)$$

We term these beams as *Werner beams*. The coherent mode representation of the equivalent $\frac{1}{2} \otimes T$ beams is given by,

$$J_W^{\frac{1}{2}, T}[\alpha] = \frac{1}{2(2T+1)} (\mathbb{1} - \alpha \vec{\sigma}^A \cdot \hat{T}^B), \quad \alpha \in \left[-\frac{T}{T+1}, 1\right]. \quad (34)$$

The beam (34), $J_W^{\frac{1}{2},T}[\alpha]$, is separable in the range $|\alpha| \leq \frac{T}{T+1}$. In equation (33), all beams corresponding to $\alpha > \frac{1}{3}$ are entangled, however, the beam (34) is entangled in the range $\frac{T}{T+1} < \alpha \leq 1$. Thus, the range of α , in which the beam (34) is entangled, shrinks as T increases. It implies that a lower dimensional entangled beam has a higher dimensional separable beam as its equivalent. Experimentally, the separable equivalent beams can be easily prepared by incoherent superposition of pure separable beams.

Separable decomposition of $J_W^{\frac{1}{2},1}[\alpha]$ for $\alpha = 0.5$

We now consider an example. At $\alpha = \frac{1}{2}$, $J_W^{\frac{1}{2},1}[\alpha]$ represents a classically entangled beam. Its equivalent beam, for $T = 1$, is, however separable. In fact, its separable expansion is given by,

$$\begin{aligned} & \frac{1}{6} [|V\rangle(V| \otimes |\psi_1\rangle(\psi_1| + |H\rangle(H| \otimes |\psi_2\rangle(\psi_2| \\ & + |- \rangle(-| \otimes |\psi_{3+}\rangle(\psi_{3+}| + |+ \rangle(+| \otimes |\psi_{3-}\rangle(\psi_{3-}| \\ & + |R\rangle(R| \otimes |\psi_{4+}\rangle(\psi_{4+}| + |L\rangle(L| \otimes |\psi_{4-}\rangle(\psi_{4-}|)] \\ & = \frac{1}{6} [\mathbb{1} - \frac{1}{2} \vec{\sigma} \cdot \vec{S}], \end{aligned} \quad (35)$$

where, the symbols have the following meaning:

$$\begin{aligned} |\pm\rangle &= \frac{1}{\sqrt{2}} \{|H\rangle \pm |V\rangle\}, \\ |R\rangle &= \frac{1}{\sqrt{2}} \{|H\rangle + i|V\rangle\}, |L\rangle = \frac{1}{\sqrt{2}} \{|H\rangle - i|V\rangle\}, \\ |\psi_1\rangle &= |LG_{01}\rangle; |\psi_2\rangle = |LG_{0-1}\rangle \\ |\psi_{3\pm}\rangle &= \frac{1}{2} |LG_{0-1}\rangle \pm \frac{1}{\sqrt{2}} |LG_{00}\rangle + \frac{1}{2} |LG_{01}\rangle \\ |\psi_{4\pm}\rangle &= \frac{1}{2} |LG_{0-1}\rangle \pm \frac{i}{\sqrt{2}} |LG_{00}\rangle - \frac{1}{2} |LG_{01}\rangle \end{aligned} \quad (36)$$

Thus, the beam, having the coherent mode representation $J_W^{\frac{1}{2},1}$, in the polarisation-OAM degrees of freedom can be prepared by incoherently mixing the beams as shown in equation (35). Similar separable expansions can be made for $J_W^{\frac{1}{2},T}[\alpha]$ for higher values of T . The advantage in the preparation of these beams is that there is no need of engineering spin-orbit coupling, which is needed for $J^{1/2,1/2}[\alpha]$ for the same value of α .

We now turn our attention to the applications of equivalent separable beams for transferring the information between two degrees of freedom of a beam.

5. APPLICATION: PROTOCOL FOR TRANSFER OF INFORMATION FROM ONE DEGREE OF FREEDOM TO ANOTHER

In this section, we present a protocol for transfer of information from one degree of freedom of a classical light to another degree of freedom, without using classical entanglement. The information need not be a-priori known.

In the protocol, the separable beam, having the coherent mode representation,

$$J^{BC}(\alpha)^{1/2,T} \equiv \frac{1}{2(2S+1)} (\mathbb{1} - \alpha \vec{\sigma}^B \cdot \hat{T}^C), \quad (37)$$

in, say, polarisation and OAM degrees of freedom, acts as a channel. The symbols B and C stand for polarisation and OAM degrees of freedom respectively. Note that the OAM subspace is

spanned by $(2T+1)$ OAM modes. For a given α , the minimum value of T , for which the beam, represented by $J^{BC}(\alpha)^{1/2,T}$, is separable, is given by the closest half-integer or integer greater than,

$$T_{\min} = \frac{|\alpha|}{1-|\alpha|}. \quad (38)$$

Let $J^A = \frac{1}{2}(\mathbb{1} + \vec{\sigma}^A \cdot \vec{p})$ be the coherent mode representation of an unknown beam in some degree of freedom, say path, whose equivalent is to be prepared (say, in the OAM domain). The combined coherent mode representation in the three degrees of freedom is given by,

$$J^A \otimes J^{BC}(\alpha)^{1/2,T} = \frac{1}{2^2(2T+1)} (\mathbb{1} + \vec{\sigma}^A \cdot \vec{p}) \otimes (\mathbb{1} - \alpha \vec{\sigma}^B \cdot \hat{T}^C). \quad (39)$$

There is a shared correlation between polarisation and OAM degrees of freedom, which is reflected in the structure of $J^{BC}(\alpha)^{1/2,T}$. The protocol is as follows:

1. Unlike in quantum mechanics, which is intrinsically probabilistic, the outcome of a measurement in the classical optical domain is deterministic. Hence, the experimenter may simply measure $|\psi_1\rangle = \frac{1}{\sqrt{2}}\{|0\rangle_A|V\rangle - |1\rangle_A|H\rangle\}$. Due to this measurement, the intensity of the beam gets reduced to one-fourth of its initial value and the information of path degree of freedom (A) gets transferred to the OAM degree of freedom (C). This constitutes a significant simplification over quantum teleportation since no post-processing is required. The beam, after the measurement, in the OAM degree of freedom is described by,

$$\tilde{J}^C(\alpha) \equiv \frac{1}{2T+1} (\mathbb{1} + \alpha \hat{T}^C \cdot \vec{p}). \quad (40)$$

Since the separable equivalent beam of the pure maximally entangled beam (corresponding to $\alpha = 1$) belongs to the infinite dimensional space, the beam prepared in the OAM degree of freedom is not the exact equivalent of the two-dimensional beam in the path degree of freedom. It can, however, be as close to the exact equivalent beam as desirable by choosing larger and larger values of T .

2. However, if per chance, the experimenter measures any of the other three Bell beams, the intensity will get diminished to one-fourth of its initial value as before. Additionally, it also requires a post-processing (for which no classical communication is required). If the experimenter measures one of the following three Bell beams,

$$\begin{aligned} |\psi_2\rangle &= \frac{1}{\sqrt{2}} \{|0\rangle_A|H\rangle - |1\rangle_A|V\rangle\}; \\ |\psi_3\rangle &= \frac{1}{\sqrt{2}} \{|0\rangle_A|H\rangle + |1\rangle_A|V\rangle\}; \\ |\psi_4\rangle &= \frac{1}{\sqrt{2}} \{|0\rangle_A|V\rangle + |1\rangle_A|H\rangle\}, \end{aligned} \quad (41)$$

on the path and polarisation degree of freedom, the transformations to be applied on the OAM degree of freedom are $R_1^C(\pi), R_2^C(\pi), R_3^C(\pi)$, in order. The symbols $R_1^C(\pi), R_2^C(\pi), R_3^C(\pi)$ represent analogue of Wigner rotation matrices in $(2T+1)$ -dimensional Hilbert space about \hat{e}_1, \hat{e}_2 , and \hat{e}_3 axes through an angle π in the OAM domain, i.e., $R_{\hat{n}}^C(\pi) = e^{i\vec{T}^C \cdot \hat{n}\pi}$.

¹The Pauli operators in the polarisation domain are defined as follows: $\sigma_1^B = |H\rangle\langle V| + |V\rangle\langle H|$, $\sigma_2^B = -i|H\rangle\langle V| + i|V\rangle\langle H|$, and, $\sigma_3^B = |H\rangle\langle H| - |V\rangle\langle V|$. Similarly, they can be defined in the path degrees of freedom (A), by identifying $|0\rangle_A$ and $|1\rangle_A$ to be orthonormal coherent modes of σ_3^A with eigenvalues ± 1 .

The Bell measurements can be performed experimentally in the path and polarisation degrees of freedom by employing Sagnac interferometers and a half wave plate, exactly in the same way as they have been performed in [52]. The unitary transformations (Wigner rotations) on the OAM modes can be performed by using holographic techniques proposed in [47].

In summary, the advantage of the proposed protocol is that it does not require a classically entangled beam as a channel. The channel is also mixed and, hence, is relatively easier to produce. This concludes our discussion of application of equivalent separable beams in an information-transfer protocol.

6. INFORMATION TRANSFER WITH MIXED 2×2 WERNER BEAMS

We have, so far, focused on manipulations of equivalents of pure beams which have a pre-determined mixedness in the given dimension (in section (4)). In this section, we address the question as to what would happen, for example, to the information transfer, if a beam of higher degree of mixedness is employed in a given dimension, as a channel. This question is pertinent because in most of the scenarios, information transfer is sought to be accomplished by using pure classically entangled light².

To address this, we investigate information transfer between different degrees of freedom, by taking the example of 2×2 Werner beams, with varying degrees of mixedness. We show that increasing mixedness (noise) is not a major impediment so long as the detector is sufficiently sensitive. That is, we argue that the same task can be accomplished by using highly mixed separable Werner beams. Crucially, retrieval of the transferred information is limited entirely by the sensitivity of the detector.

In the protocol, the channel consists of a separable $2 \otimes 2$ Werner beam (channel), having the coherent mode representation,

$$J^{BC}(\alpha)^{1/2,1/2} \equiv \frac{1}{4}(\mathbb{1} - \alpha \vec{\sigma}^B \cdot \vec{\sigma}^C), \quad \alpha \in \left[-\frac{1}{3}, 1\right], \quad (42)$$

in polarisation and OAM degrees of freedom. The beam $J^{BC}(\alpha)^{1/2,1/2}$ is separable in the range $\alpha \in \left[-\frac{1}{3}, \frac{1}{3}\right]$. The superscripts B and C stand for polarisation and OAM respectively. The parameter α is an inverse measure of noise in the channel; $\alpha = 0$ corresponds to the completely noisy channel, whereas $\alpha = 1$ corresponds to the pure channel.

Let $J^A = \frac{1}{2}(\mathbb{1} + \vec{\sigma}^A \cdot \vec{p})$ be the coherent mode representation of an unknown beam in the path degree of freedom, whose information content, encoded in \vec{p} , is to be transferred to the OAM domain. The combined coherent mode representation of the three degrees of freedom is given by,

$$J^A \otimes J^{BC}(\alpha)^{1/2,1/2} = \frac{1}{2^3}(\mathbb{1} + \vec{\sigma}^A \cdot \vec{p}) \otimes (\mathbb{1} - \alpha \vec{\sigma}^B \cdot \vec{\sigma}^C). \quad (43)$$

There is a shared correlation between the polarisation and OAM degrees of freedom, which is reflected in $J^{BC}(\alpha)^{1/2,1/2}$. The protocol is as follows:

1. Unlike in quantum mechanics, which is intrinsically probabilistic, the experimenter may simply measure $|\psi_1\rangle = \frac{1}{\sqrt{2}}(|0\rangle_A|V\rangle - |1\rangle_A|H\rangle)$. Due to this measurement, the intensity of the beam gets reduced to one-fourth of its initial

value and the information of path degree of freedom (A) gets transferred to the OAM degree of freedom (C). This constitutes a significant simplification over quantum teleportation that no post-processing is required. The beam, after the measurement, in the OAM degree of freedom is given by,

$$\tilde{J}^C(\alpha) \equiv \frac{1}{2}(\mathbb{1} + \alpha \vec{\sigma}^C \cdot \vec{p}). \quad (44)$$

2. However, if per chance, the experimenter measures any of the other three Bell beams, the intensity will get diminished to one-fourth of its initial value as before. Additionally, it also requires a post-processing (for which no classical communication is required). If the experimenter measures one of the following three Bell beams,

$$\begin{aligned} |\psi_2\rangle &= \frac{1}{\sqrt{2}}\{|0\rangle_A|H\rangle - |1\rangle_A|V\rangle\}; \\ |\psi_3\rangle &= \frac{1}{\sqrt{2}}\{|0\rangle_A|H\rangle + |1\rangle_A|V\rangle\}; \\ |\psi_4\rangle &= \frac{1}{\sqrt{2}}\{|0\rangle_A|V\rangle + |1\rangle_A|H\rangle\}, \end{aligned} \quad (45)$$

on the path and polarisation degree of freedom, the transformations to be applied on the OAM degree of freedom are $\sigma_1^C, \sigma_2^C, \sigma_3^C$, in order.

This brings out a fundamental difference between quantum and classical teleportation. The measurement in the former is probabilistic, whereas, in the latter, is deterministic. As a consequence, the post-processing (application of unitary operations) is generically unavoidable in the quantum teleportation protocols. In the example considered above, the measurement corresponding to $|\psi_1\rangle$ does away with any post-processing.

The unitary transformations on the OAM modes, corresponding to the measurement of $|\psi_2\rangle, |\psi_3\rangle$ and $|\psi_4\rangle$ can be performed using holographic techniques proposed in [47]. The Bell measurements can be performed in the path and polarisation degrees of freedom by employing Sagnac interferometers and a half wave plate, which performs a CNOT gate operation, as has been discussed in detail in [52].

Thus, following the protocol, the information encoded in \vec{p} (in the path degree of freedom) is transferred to the other degree of freedom (OAM). The crucial step is the retrieval of this information. We discuss the retrieval of information from $\tilde{J}_1^C(\alpha)$ in the next subsection.

A. Retrieval of information in the OAM degree of freedom

We observe from the equation (44) that the effect of noise (i.e., α) is reflected in diminution of \vec{p} to $\alpha\vec{p}$, when the information is transferred from the path to the OAM degree of freedom. Thanks to the experimental advances, this is not a major disadvantage since the process of information retrieval has become considerably simpler. Speaking algebraically, in order to retrieve the information, a measurement of $\vec{\sigma}^C \cdot \hat{n}$ is to be performed, followed by a normalisation with respect to α (the case $\alpha = 0$ is a singularity from which no information retrieval is possible). This would offset the diminution due to noise. Thus, howsoever small the value of α be, the measurement of a corresponding observable $\frac{1}{\alpha}\vec{\sigma}^C \cdot \hat{n}$, in principle, may be employed to extract the information of \vec{p} .

In practice, note that a small value of α corresponds to a decreased signal-to-noise ratio. The measurement of $\frac{1}{\alpha}\vec{\sigma}^C \cdot \hat{n}$ is limited exclusively by the resolution of the detector. Thus, so

²In most of the scenarios, state transfer from one degree of freedom to another, by employing pure classically entangled light, is aimed at transferring information from the former to the latter.

long as a detector with sufficient resolution is available, this protocol may be employed to transfer information even with noisy beams, which are separable as well.

We work out an explicit example. A natural measure of information in a light beam is the variation in the pattern against a background corresponding to the completely mixed channel. Let the two-dimensional OAM subspace be spanned by the modes $|LG_{00}\rangle$ and $|LG_{01}\rangle$ and $\vec{p} = (\sin \theta, 0, \cos \theta)^T$. Then, the coherent mode representation of the beam in two-dimensional subspace of OAM degree of freedom is,

$$\frac{1}{2}(\mathbb{1} + \alpha \vec{\sigma}_3 \cdot \vec{p}) \equiv \frac{1+\alpha}{2}|\psi\rangle\langle\psi| + \frac{1-\alpha}{2}|\psi_2\rangle\langle\psi_2|, \quad (46)$$

where the beams $|\psi_1\rangle$ and $|\psi_2\rangle$ are given by,

$$\begin{aligned} |\psi_1\rangle &= \cos \frac{\theta}{2} |LG_{00}\rangle + \sin \frac{\theta}{2} |LG_{01}\rangle, \\ |\psi_2\rangle &= -\sin \frac{\theta}{2} |LG_{00}\rangle + \cos \frac{\theta}{2} |LG_{01}\rangle. \end{aligned} \quad (47)$$

In order to highlight the effect of α on signal-to-noise ratio in the beam represented by (46), we plot the difference in intensities I_{diff} , given by,

$$\begin{aligned} I_{\text{diff}} &\equiv \frac{1+\alpha}{2} \left| \cos \frac{\theta}{2} |LG_{00}\rangle + \sin \frac{\theta}{2} |LG_{01}\rangle \right|^2 \\ &+ \frac{1-\alpha}{2} \left| -\sin \frac{\theta}{2} |LG_{00}\rangle + \cos \frac{\theta}{2} |LG_{01}\rangle \right|^2 \\ &- \frac{1}{2} (|LG_{00}|^2 + |LG_{01}|^2). \end{aligned} \quad (48)$$

The last term corresponds to the total intensity in the OAM modes when $\alpha = 0$, i.e., when the channel is completely mixed. We plot I_{diff} for three values of α , viz., 0.2, 0.4 and 0.9. Note that only $\alpha = 0.2$ corresponds to a separable beam. For each value of α , we have plotted I_{diff} for $\theta = 0, \frac{\pi}{4}, \frac{\pi}{2}, \frac{3\pi}{4}$ and π . The following two features are of significance to us:

1. Effect of variation of α for a fixed θ :

A comparison of figures (6), (7) and (8) shows that the contrast in the image increases with increase in α . We observe that the shape of the intensity-profile remains unchanged with increase in α , with the contrast being increasingly monotonic with purity of the beam. That is, the only change is in the scale of the plot. This substantiates our point that the same information can be retrieved from noisy beams provided a detector with sufficient resolution is available.

2. Effect of variation of θ for a fixed α :

For each θ , there is a characteristic pattern of I_{diff} , as may be seen from equations (6), (7) and (8). The change in the pattern with respect to θ contains information encoded in different linear combinations of $|LG_{01}\rangle$ and $|LG_{0-1}\rangle$.

We may now conclude the section by noting that a variation in α changes the contrast of the pattern, whereas a variation in θ changes the profile of the pattern. We now turn our attention to a more conventional application, viz., variational quantum algorithms.

7. VARIATIONAL QUANTUM CLASSIFIER ALGORITHMS

Recently, variational quantum algorithms have attracted a lot of attention [7–11], as they provide speedups as compared to their classical counterparts. The protocols consist of two broad

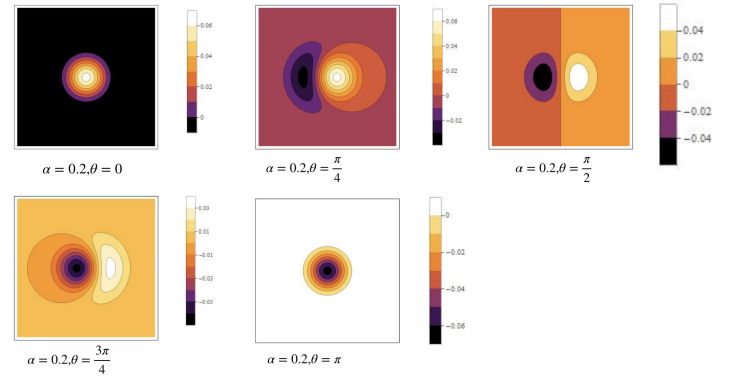


Fig. 6. Plot of I_{diff} in the transverse plane for $\alpha = 0.2$ and different values of θ . Note that the intensity profile changes with θ . The scale of the plot is of the order of 0.06.

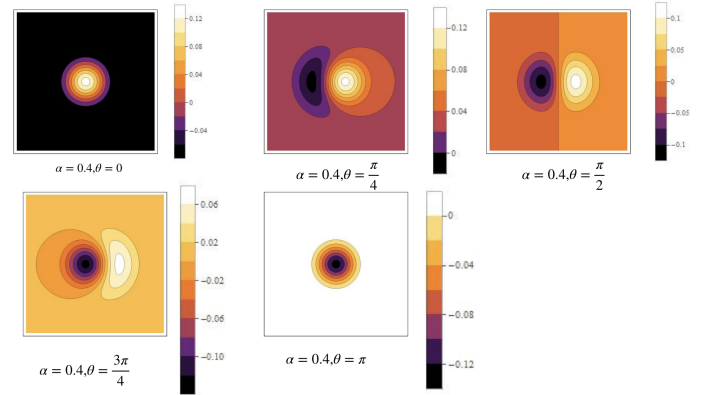


Fig. 7. Plot of I_{diff} in the transverse plane for $\alpha = 0.4$ and different values of θ . The intensity profile changes with θ . The scale of the plot is of the order of 0.12.

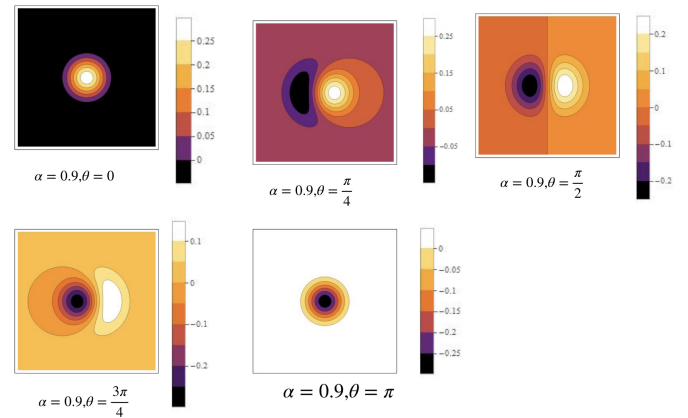


Fig. 8. Plot of I_{diff} in the transverse plane for $\alpha = 0.9$ and different values of θ . The intensity profile changes with θ . The scale of the plot is of the order of 0.25.

varieties: (I) those employing multi-qubit systems, and, (II) those employing a single quNit system (N -dimensional quantum states). The former protocols employ entangling gates, e.g., CNOT gate, Toffoli gate, etc. The latter protocols, however, do not employ entangling gates. Although the two are physically distinct, mathematically they are essentially equivalent. All the gates acting on N -qubit systems map to some operations belonging to the special unitary group of dimension $D(\equiv 2^N)$ for a qudit system of dimension D .

We first describe in brief the variational quantum classifier algorithm, proposed in [45] for a quNit system, for the purpose of illustration. For a detailed discussion of this and associated protocols, we refer the reader to [7–11, 45].

Consider a data set $S = \{(\mathbf{x}, f(\mathbf{x}))\}$. Each element of S is an ordered pair $(\mathbf{x}, f(\mathbf{x}))$, where \mathbf{x} is an input vector of arbitrary dimension and $f(\mathbf{x})$ is its associated label indicating the particular class the input belongs to. Thus, f is a mapping of each input vector to a label, belonging to a set: $\mathbb{L} = \{l_1, l_2, \dots, l_N\}$; $f: \mathbf{x} \rightarrow \mathbb{L}$. Each label corresponds to an output class, whose total number is N . Supervised learning aims at training a machine using a subset T chosen from the given dataset such that the machine can infer correct labels for the train set T as well as the test set $S - T$. That is, we require the machine to return a function f^* so that $f^*(\mathbf{x}) = f(\mathbf{x})$ for maximum number of input vectors.

A typical quantum protocol for supervised learning, that employs variational algorithms, can be divided into the following three stages:

A. State preparation in the quantum domain

To initialise the protocol, let there be a single quNit belonging to the N -dimensional Hilbert space \mathcal{H}^N . It is ensured that the dimension of the Hilbert space is equal to the cardinality of \mathbb{L} , i.e., the total number of output classes. This is essential for the scheme proposed in [45]. The input vectors, \mathbf{x} , will be represented in \mathcal{H}^N by $|\psi(\mathbf{x})\rangle$. The encoding scheme employed to obtain $|\psi(\mathbf{x})\rangle$ is given as,

$$|\psi(\mathbf{x})\rangle = e^{i\bar{S}_3(\sum_{j=1}^d w_j x_j)} H^{(N)} |0\rangle \quad (49)$$

$$\equiv Z(w_1, w_2, \dots, w_d) H^{(N)} |0\rangle$$

Here, x_j represents the j -th component of the input vector \mathbf{x} , \bar{S}_3 is the diagonal matrix $\text{diag}(-(N-1)/2, \dots, (N-1)/2)$, $|0\rangle = (1, 0, 0, \dots, 0)^T$ and $H^{(N)}$ is the generalized Hadamard gate.

The variables $\{w_i; i = 1, 2, \dots, d\}$ are free parameters that can be tuned, during training. It is, thus, a parameter dependent state preparation procedure.

B. Parametrized unitary operations in the quantum domain

Input vectors \mathbf{x} are encoded in states of a single quNit. The most general unitary operation that can be applied to such a state belongs to the $SU(N)$ group. Since the group $SU(N)$ has $N^2 - 1$ generators, the most general unitary transformation belonging to it admits a generalised Euler angle parametrisation as [53]:

$$U(N)(\{\alpha_j\}) = e^{i\lambda_1 \alpha_1} e^{i\lambda_2 \alpha_2} \dots e^{i\lambda_{(N^2-1)} \alpha_{(N^2-1)}}. \quad (50)$$

The set $\{\alpha_j; j = 1, 2, \dots, N^2 - 1\}$ constitutes a set of learnable parameters while the set $\{\lambda_j\}$ consists of the standard generators of $SU(N)$.

C. Measurement and decision functions in the quantum domain

The final stage of the algorithm involves prediction of the label for an input vector by the classifier. In [45], this decision making is determined by a projective measurement on the transformed state $|\tilde{\psi}(\mathbf{x})\rangle = U(N)|\psi(\mathbf{x})\rangle$ in the basis $\{|0\rangle, \dots, |N-1\rangle\}$. Thus, measurement of any non-degenerate operator, say, $A = \sum_{a=0}^{N-1} a|a\rangle\langle a|$ in this basis may be employed.

In order to predict the label associated with \mathbf{x} , the complete set of probabilities $\{p_a = \text{Tr}(\pi_a |\tilde{\psi}(\mathbf{x})\rangle\langle\tilde{\psi}(\mathbf{x})|)\}$, corresponding to all outcomes, for the state $|\tilde{\psi}(\mathbf{x})\rangle$ would have to be constructed. The following rule is stipulated:

$$p_b = \max\{p_a\} \rightarrow f^*(\mathbf{x}) = l_b, \quad (51)$$

i.e., the predicted label will be l_b iff $S_3 = b$ is the most likely outcome of the measurement. The predicted label is not necessarily the same as actual label. Hence to minimize mismatches, one needs to train the circuit. A sample \mathbf{x} is said to be correctly classified iff $f^*(\mathbf{x}) = f(\mathbf{x})$.

This concludes the forward part of the computation. After this, an error estimation is done with a classical computer. The training process aims at minimizing the error function E . It is carried out on a classical computer since E is a classical function. After each epoch, the training parameters $\{w_i; i = 1, 2, \dots, d\}$ and $\{\alpha_i; i = 1, 2, \dots, (N^2 - 1)\}$ are updated to minimize E , say, by using the classical gradient descent technique. This is the feedback part of the computation. After that, the forward part of the computation is carried out once again. This process is repeated until the value of E converges to a minimum. At that stage the values of the free parameters are frozen and training is complete.

8. IMPLEMENTATION OF VARIATIONAL QUANTUM CLASSIFIER ALGORITHM WITH CLASSICAL LIGHT

It is evident that due to robust generation, manipulation and detection techniques of OAM modes, quantum algorithms that require only parallelism can be simulated with classical light efficiently. In particular, we propose, in this section, how variational quantum algorithms can be implemented with OAM modes of classical light, through the example of the quantum classifier circuit discussed in the preceding section.

As before, consider the dataset $S = \{\mathbf{x}, f(\mathbf{x})\}$; $\mathbf{x} \in \mathbb{R}^d$, $f: \mathbf{x} \rightarrow \mathbb{L} = \{l_1, l_2, \dots, l_N\}$. \mathbb{L} is the set of labels. In what follows, we propose the setup for implementation of quantum classifier algorithm stage-by-stage by employing OAM modes:

A. Beam preparation with classical light

First of all, if $|\psi(\mathbf{x})\rangle$ (given in equation (49)) belongs to N -dimensional Hilbert space \mathcal{H}^N , we may choose N orthonormal Laguerre Gauss modes of classical light. There is no need to first prepare the beam corresponding to $|0\rangle$ (i.e., $|LG_{00}\rangle$ beam, i.e., a Laguerre-Gauss mode with both radial and azimuthal index equal to zero), followed by some transformations on it. The beam $|\psi(\mathbf{x})\rangle$ corresponding to the state $|\psi(\mathbf{x})\rangle$ (given in equation (49)) can be directly prepared. That is to say,

$$|\psi(\mathbf{x})\rangle = \sum_i \mu_i |\psi_i\rangle \mapsto \sum_i \mu_i |LG_{0i}\rangle. \quad (52)$$

Recall that $|LG_{0i}\rangle$ represents a classical beam with OAM mode index equal to ' i ' and radial mode index equal to 0.

B. Parametrized unitary operations with classical light

The tunable unitary transformations on the OAM modes can be performed by using holographic techniques proposed in [47]. This method allows, in principle, the implementation of any unitary transformation on the OAM modes. To describe briefly, the input beam, which is already in a superposition of OAM modes, passes through a hologram, designed to perform the desired transformation. Thereafter, a second hologram reduces the cross-talk between different modes. If there are N modes involved, the lower bound on efficiency of this technique is found to be $\frac{1}{N^{3/2}}$ [47].

C. Measurement and decision functions with classical light

We shall now show how the task of measurements and determination of decision functions can be accomplished with OAM modes. First, we perform a log-polar transform on the OAM beam, emergent from the tunable hologram, so that intensity, corresponding to each Laguerre-Gauss mode, is distributed in the transverse direction. It can be captured via a charge coupled device (CCD). The normalised intensity is formally analogous to the quantum probability. Hence, equation (51) translates to the fact that the mode corresponding to b (in equation (51)) has the greatest intensity. The output of that CCD is given as a feedback to the computer that creates the pattern for spatial light modulator.

The backward part of the computation is performed on a classical computer whether the protocol is implemented on a classical or a quantum platform. So, it requires no additional setup in this case. The same steps, as discussed in the previous section, would do the job in this case as well.

We have, so far, shown a setup for a protocol, originally proposed for a qubit system. However, many variational algorithms have been proposed for N -qubit systems. We outline the procedure for their implementation with OAM modes of classical light. Obviously, the composite N -qubit system in these algorithms belongs to a 2^N -dimensional Hilbert space. Furthermore, these algorithms also employ various gate operations with tunable parameters. Thanks to isomorphism of vector spaces of identical dimensions, the corresponding gates can be identified for a single qudit system of identical dimensions (i.e., 2^N).

As an example, if we consider a two-qubit system, the most general transformation acting on it belongs to $SU(4)$. A natural choice of basis for the operators is as follows:

$$\{\mathbb{1}, \sigma_{1\alpha} \otimes \mathbb{1}, \mathbb{1} \otimes \sigma_{2\beta}, \sigma_{1\alpha} \otimes \sigma_{2\beta}\}; \alpha, \beta \in \{1, 2, 3\}. \quad (53)$$

One may first make the following mapping of the basis elements from the Hilbert space of a two-qubit to the Hilbert space of a single four-level system:

$$|i_1 i_0\rangle \mapsto |2i_1 + i_0\rangle; i_0, i_1 \in \{0, 1\}. \quad (54)$$

With this mapping, all the states, observables and transformation matrices get mapped from the two-qubit systems to a single four-level system. This procedure admits straightforward generalisation to N -qubit systems.

Thus, the implementation of these protocols with OAM modes is a two-step process. First, the basis vectors of tensor product of N two-dimensional Hilbert spaces should be mapped to those of the 2^N -dimensional Hilbert space of a single qudit. Secondly, the basis vectors of 2^N -dimensional Hilbert space can be mapped to 2^N OAM modes of classical light.

This example shows that there is a class of machine learning algorithms for different tasks that can be implemented by

employing OAM modes of classical light. We have discussed but one particular example. Of course, implementations of tunable unitary transformations become challenging with increase in dimensions of Hilbert space (i.e., the number of modes involved). The modes have to be chosen in such a way that their patterns can be resolved after log-polar transformation. Nevertheless, the need for both—a single photon source and a single photon detector, that are quintessential for implementation of the protocols on a quantum platform—is eliminated. Additionally, the simulability of variational algorithms with OAM modes provides a motivation for engineering of such devices that can robustly perform tunable transformations.

9. CONCLUSION

In conclusion, we have put forth a new class of beams, termed as *equivalent beams*. Employing these beams, we have proposed a protocol for transfer of information from one degree of freedom of a classical beam to another without the need for classical entanglement. Production of equivalent beams is not experimentally difficult [22]. The advantage of the protocol is that the information processing can be done with highly mixed beams as one employs higher dimensionality. We have next considered variational quantum algorithms, and shown a setup for their implementation with OAM modes of light.

This work shows that there are many so-called quantum phenomena that can be simulated with classical light. With the availability of robust generation, manipulation and detection techniques, OAM modes offer versatile platform to perform these tasks, at times even without classical entanglement. The setups for many other quantum phenomena and algorithms will be proposed in a separate paper.

ACKNOWLEDGEMENT

We thank Rajni Bala for several discussions and helpful suggestions. Sooryansh thanks the Council for Scientific and Industrial Research (Grant no. -09/086 (1278)/2017-EMR-I) for funding his research.

DISCLOSURES

The authors declare no conflicts of interest.

REFERENCES

1. D. Deutsch, "Quantum theory, the church-turing principle and the universal quantum computer," *Proc. Royal Soc. London. Ser. A, Math. Phys. Sci.* **400**, 97 (1985).
2. D. Deutsch and R. Jozsa, "Rapid solution of problems by quantum computation," *Proc. Royal Soc. London. Ser. A: Math. Phys. Sci.* **439**, 553–558 (1992).
3. D. R. Simon, "On the power of quantum computation," *SIAM journal on computing* **26**, 1474–1483 (1997).
4. E. Bernstein and U. Vazirani, "Quantum complexity theory," *SIAM J. on Comput.* **26**, 1411–1473 (1997).
5. P. Shor, "Polynomial-time algorithms for prime factorization and discrete logarithms on a quantum computer," *SIAM J. on Comput.* **26**, 1484–1509 (1997).
6. L. K. Grover, "Quantum mechanics helps in searching for a needle in a haystack," *Phys. review letters* **79**, 325 (1997).
7. K. H. Wan, O. Dahlsten, H. Kristjánsson, R. Gardner, and M. Kim, "Quantum generalisation of feedforward neural networks," *npj Quantum information* **3**, 1–8 (2017).
8. E. Farhi and H. Neven, "Classification with quantum neural networks on near term processors," *arXiv preprint arXiv:1802.06002* (2018).

9. P. Rebentrost, T. R. Bromley, C. Weedbrook, and S. Lloyd, "Quantum hopfield neural network," *Phys. Rev. A* **98**, 042308 (2018).
10. M. Schuld and N. Killoran, "Quantum machine learning in feature hilbert spaces," *Phys. review letters* **122**, 040504 (2019).
11. V. Havlíček, A. D. Córcoles, K. Temme, A. W. Harrow, A. Kandala, J. M. Chow, and J. M. Gambetta, "Supervised learning with quantum-enhanced feature spaces," *Nature* **567**, 209–212 (2019).
12. R. Horodecki, P. Horodecki, M. Horodecki, and K. Horodecki, "Quantum entanglement," *Rev. Mod. Phys.* **81**, 865–942 (2009).
13. A. Streltsov, G. Adesso, and M. B. Plenio, "Colloquium: Quantum coherence as a resource," *Rev. Mod. Phys.* **89**, 041003 (2017).
14. A. Bera, T. Das, D. Sadhukhan, S. S. Roy, A. Sen(De), and U. Sen, "Quantum discord and its allies: a review of recent progress," *Reports on Prog. Phys.* **81**, 024001 (2017).
15. B. Amaral, "Resource theory of contextuality," *Philos. Transactions Royal Soc. A* **377**, 20190010 (2019).
16. C. Ferrie and J. Combes, "How the result of a single coin toss can turn out to be 100 heads," *Phys. Rev. Lett.* **113**, 120404 (2014).
17. L. Allen, M. Padgett, and M. Babiker, "In the orbital angular momentum of light," *Prog. optics* **39**, 291–372 (1999).
18. D. L. Andrews and M. Babiker, *The angular momentum of light* (Cambridge University Press, 2012).
19. L. Allen and M. Padgett, "The orbital angular momentum of light: An introduction," *Twist. Photons: Appl. Light. with Orbital Angular Momentum* pp. 1–12 (2011).
20. L. Marrucci, E. Karimi, S. Slussarenko, B. Piccirillo, E. Santamato, E. Nagali, and F. Sciarrino, "Spin-to-orbital conversion of the angular momentum of light and its classical and quantum applications," *J. Opt.* **13**, 064001 (2011).
21. Y. Shen, X. Wang, Z. Xie, C. Min, X. Fu, Q. Liu, M. Gong, and X. Yuan, "Optical vortices 30 years on: Oam manipulation from topological charge to multiple singularities," *Light. Sci. & Appl.* **8**, 1–29 (2019).
22. P.-H. Tuan, H.-C. Liang, K.-F. Huang, and Y.-F. Chen, "Realizing high-pulse-energy large-angular-momentum beams by astigmatic transformation of geometric modes in an nd: Yag/cr4+: Yag laser," *IEEE J. Sel. Top. Quantum Electron.* **24**, 1–9 (2018).
23. L. Mandel and E. Wolf, *Optical coherence and quantum optics* (Cambridge university press, 1995).
24. H. Sztul and R. Alfano, "Double-slit interference with laguerre-gaussian beams," *Opt. letters* **31**, 999–1001 (2006).
25. E. Wolf, *Introduction to the Theory of Coherence and Polarization of Light* (Cambridge University Press, 2007).
26. A. K. Jha, J. Leach, B. Jack, S. Franke-Arnold, S. M. Barnett, R. W. Boyd, and M. J. Padgett, "Angular two-photon interference and angular two-qubit states," *Phys. review letters* **104**, 010501 (2010).
27. M. Malik, S. Murugkar, J. Leach, and R. W. Boyd, "Measurement of the orbital-angular-momentum spectrum of fields with partial angular coherence using double-angular-slit interference," *Phys. Rev. A* **86**, 063806 (2012).
28. L. Allen, M. W. Beijersbergen, R. J. C. Spreeuw, and J. P. Woerdman, "Orbital angular momentum of light and the transformation of laguerre-gaussian laser modes," *Phys. Rev. A* **45**, 8185–8189 (1992).
29. A. Forbes, A. Aiello, and B. Ndagano, "Classically entangled light," *Prog. Opt.* **64**, 99–153 (2019).
30. S. M. Hashemi Rafsanjani, M. Mirhosseini, O. S. Magaña Loaiza, and R. W. Boyd, "State transfer based on classical nonseparability," *Phys. Rev. A* **92**, 023827 (2015).
31. T. Li, X. Zhang, Q. Zeng, B. Wang, and X. Zhang, "Experimental simulation of monogamy relation between contextuality and nonlocality in classical light," *Opt. Express* **26**, 11959–11975 (2018).
32. S. K. Goyal, F. S. Roux, A. Forbes, and T. Konrad, "Implementing quantum walks using orbital angular momentum of classical light," *Phys. Rev. Lett.* **110**, 263602 (2013).
33. M. D. Eisaman, J. Fan, A. Migdall, and S. V. Polyakov, "Invited review article: Single-photon sources and detectors," *Rev. scientific instruments* **82**, 071101 (2011).
34. P. R. Hemmer, A. Muthukrishnan, M. O. Scully, and M. S. Zubairy, "Quantum lithography with classical light," *Phys. Rev. Lett.* **96**, 163603 (2006).
35. G. Kaur, G. Narang *et al.*, "Optical implementations, oracle equivalence, and the Bernstein-Vazirani algorithm," *JOSA B* **24**, 221–225 (2007).
36. P. B. Dixon, D. J. Starling, A. N. Jordan, and J. C. Howell, "Ultrasensitive beam deflection measurement via interferometric weak value amplification," *Phys. Rev. Lett.* **102**, 173601 (2009).
37. D. P. Atherton, G. Ranjit, A. A. Geraci, and J. D. Weinstein, "Observation of a classical cheshire cat in an optical interferometer," *Opt. Lett.* **40**, 879–881 (2015).
38. B. Perez-Garcia, M. McLaren, S. K. Goyal, R. I. Hernandez-Aranda, A. Forbes, and T. Konrad, "Quantum computation with classical light: Implementation of the Deutsch–Jozsa algorithm," *Phys. Lett. A* **380**, 1925 – 1931 (2016).
39. B. Perez-Garcia, R. I. Hernandez-Aranda, A. Forbes, and T. Konrad, "The first iteration of grover's algorithm using classical light with orbital angular momentum," *J. Mod. Opt.* **65**, 1942–1948 (2018).
40. T. Konrad and A. Forbes, "Quantum mechanics and classical light," *Contemp. Phys.* **60**, 1–22 (2019).
41. S. Zhang, P. Li, B. Wang, Q. Zeng, and X. Zhang, "Implementation of quantum permutation algorithm with classical light," *J. Phys. Commun.* **3**, 015008 (2019).
42. H. Chevalier, A. J. Paige, H. Kwon, and M. S. Kim, "Violating the leggett-garg inequalities with classical light," *Phys. Rev. A* **103**, 043707 (2021).
43. H. M. Bharath and V. Ravishankar, "Classical simulation of entangled states," *Phys. Rev. A* **89**, 062110 (2014).
44. S. Asthana, R. Bala, and V. Ravishankar, "Quantum communication with SU(2) invariant separable $2 \times N$ level systems," *arXiv preprint arXiv:2104.04469* (2021).
45. S. Adhikary, S. Dangwal, and D. Bhowmik, "Supervised learning with a quantum classifier using multi-level systems," *Quantum Inf. Process.* **19**, 1–12 (2020).
46. K. Zhang, Y. Wang, Y. Yuan, and S. N. Burokur, "A review of orbital angular momentum vortex beams generation: from traditional methods to metasurfaces," *Appl. Sci.* **10**, 1015 (2020).
47. Y. Wang, V. Potoček, S. M. Barnett, and X. Feng, "Programmable holographic technique for implementing unitary and nonunitary transformations," *Phys. Rev. A* **95**, 033827 (2017).
48. R. J. C. Spreeuw, "Classical wave-optics analogy of quantum-information processing," *Phys. Rev. A* **63**, 062302 (2001).
49. L. D. Landau and E. M. Lifshitz, *The classical theory of fields*, vol. 2, pp 119-124 (Pergamon Press, 1971).
50. S. Adhikary, I. K. Panda, and V. Ravishankar, "Super-quantum states in SU(2) invariant level systems," *Annals Phys.* **377**, 87–95 (2017).
51. J. M. Radcliffe, "Some properties of coherent spin states," *J. Phys. A: Gen. Phys.* **4**, 313–323 (1971).
52. D. Guzman-Silva, R. Brünig, F. Zimmermann, C. Vetter, M. Gräfe, M. Heinrich, S. Nolte, M. Duparré, A. Aiello, M. Ornigotti *et al.*, "Demonstration of local teleportation using classical entanglement," *Laser & Photonics Rev.* **10**, 317–321 (2016).
53. M. Byrd and E. C. G. Sudarshan, "SU(3) revisited," *J. Phys. A: Math. Gen.* **31**, 9255–9268 (1998).